Validation of Vector Magnitude Datasets: Effects of Random Component Errors

MICHAEL H. FREILICH

College of Oceanic and Atmospheric Sciences, Oregon State University, Corvallis, Oregon

(Manuscript received 18 March 1996, in final form 6 November 1996)

ABSTRACT

A statistically consistent and physically realistic approach for validating vector magnitude measurements is developed, based on a model for random measurement noise that explicitly satisfies a nonnegativity constraint for all ''noisy'' vector magnitude measurements. Numerical and analytic approximations are used to quantify the nonlinear functional dependence of sample conditional means on true values and component noise magnitudes. In particular, it is shown analytically that random component errors will result in overall vector magnitude biases. A simple nonlinear regression of measured sample conditional mean vector magnitudes (calculated from traditional collocated data) against Monte Carlo simulation results is proposed for determining both deterministic trends and random errors in the data to be validated. The approach is demonstrated using Seasat and *ERS-1* scatterometer measurements and collocated buoy data. The approach accounts well for the observed qualitative features of the collocated datasets and yields realistic values of random component error magnitudes and deterministic gain and offset for each dataset. An apparent systematic insensitivity of scatterometers at low wind speeds is shown to be a consequence of random component speed errors if it is assumed that the comparison buoy measurements are error free.

1. Introduction

Many satellite remote sensing measurement techniques are highly indirect, necessitating extensive postlaunch calibration and algorithm refinement. Construction of consistent, accurate, climate datasets thus requires careful validation of the satellite measurements, especially for the many oceanographic and climate studies requiring multidecadal time series that exceed the lifetime of single instruments. Such validation historically has relied upon comparisons between the satellite measurements and independent temporally and spatially collocated data of presumably known accuracy.

Although the crucial importance of accurate validation has long been recognized, the oceanographic and remote sensing communities have demonstrated surprisingly little appreciation for the problem's statistical complexities. These complexities increase when the geophysical quantity of interest is a vector or a vector-related scalar (such as a vector magnitude). This paper addresses several issues related specifically to validation of wind speed (rather than vector velocity) measurements through comparisons with collocated in situ or previously calibrated data. While the problem is cast in terms of validating scatterometer wind speed estimates, the results also apply to other instruments that measure vector magnitudes, provided that their processing algorithms are constrained to produce only physically realistic nonnegative magnitudes.

Satellite-borne microwave scatterometers can be used to estimate near-surface wind velocity over the oceans under clear-sky and cloudy conditions (see Naderi et al. 1991 for a review of scatterometry). Extensive ground-based processing of the direct scatterometer cross-sectional measurements is required to extract wind velocity information, and even then selection of a unique direction is often difficult owing to instrumental noise and model function uncertainties (Naderi et al. 1991). Basic scatterometer processing can, however, yield relatively accurate estimates of wind speed even though uncertainties in wind direction remain. It is thus understandable that many historical and planned scatterometer validation efforts focus initially on scalar wind speed rather than component amplitudes or full vector velocities.

Three main factors complicate wind speed validations. Most fundamentally, wind speed is the magnitude of a vector. Although the simplest probabilistic model for wind speed measurements would involve Gaussian errors, all physically realistic wind speed estimates must be nonnegative, and it is not possible to interpret noisy wind speed measurements simply as everywhere nonnegative ''true'' speeds contaminated by additive Gaussian noise. Second, global ocean wind speeds (and representative validation datasets) are neither normally nor uniformly distributed. The normal distribution is precluded by the nonnegative property of speeds, while

Corresponding author address: Michael H. Freilich, College of Oceanic and Atmospheric Sciences, Oregon State University, 104 Ocean Admin Building, Corvallis, OR 97331-5503.
E-mail: mhf@oce.orst.edu

globally representative validation datasets are dominated by measurements corresponding to a midrange of wind speeds. Analytic simplifications afforded by the uniform or Gaussian distributions thus cannot be exploited.

Finally, both the satellite measurements to be validated and the comparison data used as the validation standard generally contain errors or are not fully compatible. For example, buoy measurements are often fixed-length temporal averages at a single location, while scatterometer measurements are near-instantaneous spatial averages. Spatial and temporal inhomogeneities in the true wind field lead to differences between the two measurements, even if both are ''perfect.'' Errors and incompatibilities in the comparison measurements bias regression analyses and greatly complicate the interpretation of comparison results (Pierson 1983; Freilich 1986; Monaldo 1988; Press et al. 1992). The present work only addresses effects of nonnegative wind speeds and nonuniform distribution of true speeds on validation analysis and interpretation. Throughout this paper, it is assumed that the conventional comparison measurements (e.g., acquired by buoys) are error free. Differences resulting from incompatibilities between the spaceborne and in situ comparison measurements are considered as errors in the spaceborne measurements. Ongoing investigations of the impact of errors in the comparison data will be reported elsewhere.

This paper is organized as follows. Simple yet realistic models for true wind speeds and associated ''noisy'' measurements are developed in sections 2 and 3 for the random-noise-only case where deterministic calibration errors are absent. The models afford several analytic and practical simplifications; in particular, the distribution of the noisy wind speed measurements can be derived analytically and large datasets for Monte Carlo simulation analyses can be constructed efficiently. Conditional mean differences between true and noisy wind speeds are examined using numerical techniques in section 4, and the approach is generalized to accommodate linear deterministic calibration errors in section 5. The validation analysis is applied to actual comparison data from the Seasat and *ERS-1* scatterometers in section 6. Discussion and conclusions follow in section 7.

2. True wind speed distributions

Many authors have examined the climatological distribution of near-surface wind speeds. Most studies have concentrated on engineering problems (e.g., wind loading of structures and wind power generation) at land sites for which large quantities of conventional measurements exist (Essenwanger 1976; Justus et al. 1978; Stewart and Essenwanger 1978). These investigations suggest that climatological wind speeds can be accurately approximated by Weibull distributions having between one and four parameters. Wentz et al. (1984) constructed a Ku-band scatterometer model function based on the assumption that near-surface oceanic wind speeds were Rayleigh distributed. Pavia and O'Brien (1986) used a two-parameter Weibull distribution to characterize oceanic surface wind speed distributions as a function of geographic location and season. Takle and Brown (1978) discuss modifications to the Weibull distribution to incorporate occurrences of calm.

For simplicity, the present study assumes the one-parameter Rayleigh distribution (Parzen 1960; Wentz et al. 1984; Freilich and Challenor 1994) for near-surface wind speeds over the global ocean. The Rayleigh distribution is a special case of the two-parameter Weibull and is appropriate in the present context for validation datasets in which wind speed and wind direction are uncorrelated.

The magnitudes of two-dimensional vectors are Rayleigh distributed when each component amplitude is independently drawn from a zero-mean, normal distribution. If the orthogonal component amplitudes are given by u_1 and u_2, the vector magnitude s (wind speed) is defined by

$$s \equiv |\mathbf{u}| = (u_1^2 + u_2^2)^{1/2}. \tag{1}$$

When u_1, u_2 are independent $N(0, \sigma^2)$ random variables, the probability density function for s, $f_R(s; \sigma)$, is given by

$$f_R(s; \sigma) = \frac{s}{\sigma^2} \exp\left[-\frac{1}{2}\left(\frac{s}{\sigma}\right)^2\right], \qquad s > 0 \tag{2}$$

[$f_R(s; \sigma) = 0$ for $s \le 0$]. The present study examines population statistics calculated over all wind speeds and conditional statistics calculated for specific values of the true wind speed. For Rayleigh distributed winds, the population mean wind speed $\bar{s} \equiv \int_0^\infty s f_R(s; \sigma)\, ds$ is related to the component speed standard deviation σ by

$$\sigma = \left(\frac{2}{\pi}\right)^{1/2} \bar{s}. \tag{3}$$

(In the remainder of the paper, an overbar denotes the true mean calculated analytically over the entire population, while angle brackets represent a sample mean calculated from finite data.)

Data corresponding to very low ($s < s_0$) or high ($s > s_1$) true wind speeds are often excluded in practice because of suspected large errors at extreme conditions. Where such editing has been applied, it is more appropriate to calculate the truncated mean

$$\overline{s|_{s_0}^{s_1}} \equiv \int_{s_0}^{s_1} s f_R(s; \alpha)\, ds,$$

which can be derived from (2);

$$\overline{s|_{s_0}^{s_1}} = (2\sigma^2)^{1/2}\left[\left(\frac{\sqrt{\pi}}{2}\right) - \gamma\left(\frac{3}{2}, \frac{s_0^2}{2\sigma^2}\right) - \Gamma\left(\frac{3}{2}, \frac{s_1^2}{2\sigma^2}\right)\right],$$

where $\Gamma(a, b)$ and $\gamma(a, b)$ are the incomplete gamma functions (Abramowitz and Stegun 1964).

The Rayleigh assumption allows straightforward nu-

merical generation of synthetic datasets and affords several analytic simplifications. Synthetic data covering a realistic distribution of true wind speeds and vector components can be easily constructed from (1) and (3) given knowledge of $\bar{s}$. Wentz et al. (1984) examined U.S. Navy climatological atlases and concluded that the global, temporal mean wind speed at a height of 19.5 m over the oceans was 7.4 m s^{-1}. Freilich and Challenor (1994) analyzed global ocean surface products from operational numerical weather prediction centers and Northern Hemisphere open-ocean buoys and reported quantitatively similar results. It thus seems reasonable to choose $\bar{s} = 7.4$ m s^{-1} as a globally realistic value in the present study, understanding that simulation of validation datasets derived from limited geographical regions or specific seasons may require a different choice for $\bar{s}$.

As the Rayleigh distribution implies that there are no preferred directions at each speed, vector components corresponding to any wind speed $\hat{s}$ can be simulated numerically by generating uniformly distributed directions θ_i and calculating components from

$$u_{1i} = \hat{s} \sin\theta_i \tag{4a}$$

$$u_{2i} = \hat{s} \cos\theta_i. \tag{4b}$$

Importantly, while (4a) and (4b) are natural consequences of the assumption of a Rayleigh distribution for s, (4) can be used to generate realizations of component speeds corresponding to $\hat{s}$ whenever the assumption of uniformly distributed directions at $\hat{s}$ is valid, independent of the overall distribution of s.

3. Noise models and comparison statistics

It is crucial to choose a realistic model for the systematic and random errors in the measurements to be validated (referred to below as the noisy data and represented by the subscript n). In the general case, the ith noisy wind speed measurement is given by

$$s_{ni} = g(s_i) + \epsilon_i, \tag{5}$$

where g is a deterministic function and ϵ_i is a realization of a random variable. The function g models systematic errors in s_n that might result from instrument calibration errors. The random variable ϵ represents inherently random errors caused by unmeasured geophysical variables or instrumental noise. Although in many other problems ϵ can be considered independent of s, the nonnegativity of s_n in the present wind speed analysis requires that the realizations ϵ_i be drawn from populations whose moments are functions of s.

The extreme generality of (5) limits its utility and it is necessary to restrict attention to idealized cases. Wind speed validation analyses customarily aim to identify error trends in s_n that vary only slowly with s. It is thus usual to assume (at least initially) that g is a low-order polynomial. In this section, the basic properties of the noise model are developed for the random-noise-only case where $g = s$. The noise model and validation analysis approach are then generalized in section 4 to accommodate the more typical case where

$$g = \alpha_0 + \alpha_1 s. \tag{6}$$

An obvious approach for modeling noisy vector magnitudes is to assume additive, independent normally distributed random noise on each of the true components u_i, such that

$$s_n(\bar{s}, \delta) = [(u_1 + \delta_1)^2 + (u_2 + \delta_2)^2]^{1/2}, \tag{7a}$$

where

$$\delta_1, \delta_2 = N(0, \delta^2). \tag{7b}$$

The noise model (7) was chosen primarily for its conceptual simplicity and the analytic and numerical simplifications it affords. Nonetheless, it is qualitatively consistent with known instrument and geophysical noise sources. As discussed in Naderi et al. (1991) and references therein, instrumental and communication noise contaminate scatterometer backscatter cross-sectional measurements. Extensive simulations conducted in the course of the NASA scatterometer (NSCAT) instrument design suggest that individual vector wind estimates derived from realistically noisy backscatter measurements have speed and direction error distributions roughly similar to those expected from random additive component errors. In addition, the incompatibilities between scatterometer (instantaneous spatial average) and in situ (point temporal average) data lead to apparent errors in the scatterometer measurements if the in situ data are considered perfect. Pierson (1983) discusses the relationship between unresolved mesoscale wind variability and the (separate) expected wind speed and direction ''error'' distributions. While neither the instrumental nor geophysical noise sources are strictly additive as postulated here, the noise model (7) does provide a tractable and reasonable approximation to the actual noise statistics.

The most important consequence of the noise model (7) can be derived analytically. Since u_i and δ_i are realizations of independent Gaussian variables, the noisy wind components $(u_i + \delta_i)$ are $N[0, (\sigma^2 + \delta^2)]$, and thus s_n is also Rayleigh distributed with

$$\overline{s_n} = \left[\bar{s}^2 + \left(\frac{\pi}{2}\right)\delta^2\right]^{1/2}. \tag{8}$$

The noise model (7) thus implies that random component errors lead to an overall wind speed bias whose magnitude is related to both the true mean wind speed and the variance of the (zero mean) random component errors.

Construction of realistic simulated data requires choosing appropriate component error standard deviations (δ). Wind speed validation typically involves calculation and analysis of the differences between spatially and temporally collocated measurements;

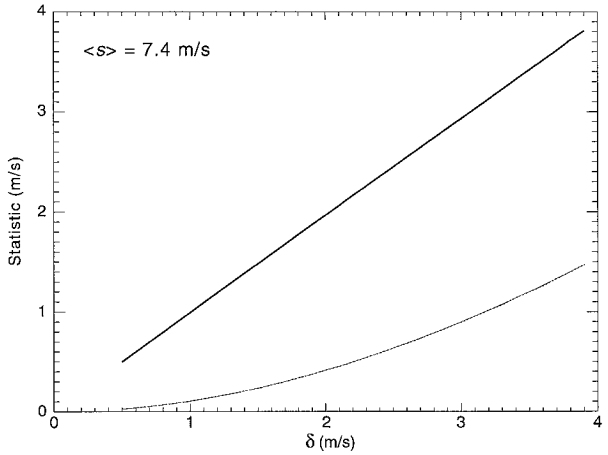

FIG. 1. Overall mean (dotted) and rms (heavy solid) wind speed difference as a function of random noise magnitude δ, based on numerical simulations and the random-noise-only model [Eqs. (7a), (7b)]. Also shown (light solid line) is the analytic overall mean derived from Eqs. (7) and (8).

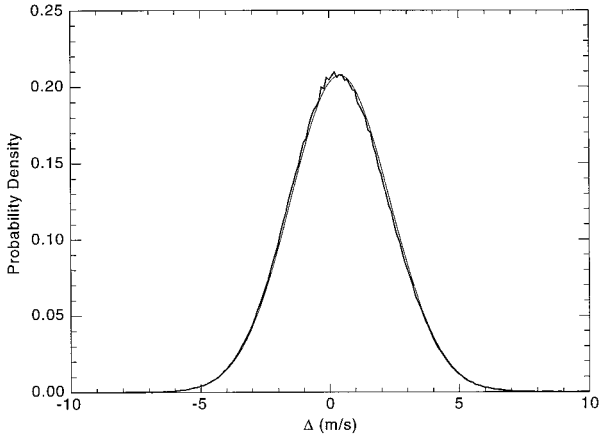

FIG. 2. Overall distribution of $\Delta \equiv s_n - s$ for the random-noise-only case with $\bar{s} = 7.4$ m s^{-1} and $\delta = 2$ m s^{-1}, based on numerical simulations (heavy line). The dashed line shows the best-fit Gaussian distribution, corresponding to $\overline{\Delta} = 0.41$ m s^{-1} and a standard deviation of 1.92 m s^{-1}.

$$\Delta_i \equiv s_{ni} - s_i. \tag{9}$$

Although the overall mean bias $\overline{\Delta}$ can be calculated analytically from (8) if δ is known, analytic forms for second-order statistics such as var[Δ] or root-mean-square differences (rms[Δ] $\equiv (\overline{\Delta^2})^{1/2}$) cannot be obtained. Estimates of the dependences of $\overline{\Delta}$ and rms[Δ] on δ were therefore calculated from a series of numerical simulations each composed of 1×10^6 pairs [$s_{ni}(\sigma, \delta)$, $s_i(\sigma)$]. The value for σ was chosen to correspond to a true mean wind speed of 7.4 m s^{-1} for each simulation using (3), while δ was varied between simulations in increments of 0.1 between 0.5 and 4.0 m s^{-1}. As shown in Fig. 1, $\langle\Delta\rangle$ estimated from the numerical simulations was identical to the analytic result (8) confirming that random component errors lead to an overall bias in the noisy wind speeds and establishing the statistical validity of the simulations. The numerical experiments also indicated (fortuitously) that rms[Δ] $\approx \delta$ for $\bar{s} = 7.4$ m s^{-1} as shown by the heavy solid line in Fig. 1.

The synthetic datasets can also shed light on the general realism of the noise model (7). While little credible work has been published regarding details of scatterometer wind speed errors, simple sample mean and rms differences calculated over the full measured range of s are often used to characterize comparisons between remotely sensed and conventionally measured wind speeds. These statistics are sufficient if, after removing systematic errors, the random differences are normally distributed, but their interpretation is not clear if the difference distribution is significantly non-Gaussian.

The synthetic datasets were used to examine the distribution of errors (over all true wind speeds) and hence the interpretation of overall bias and rms difference statistics for the error model (7). As shown in Fig. 2 for $\bar{s} = 7.4$ m s^{-1} and $\delta = 2$ m s^{-1}, the overall distribution of Δ is nearly Gaussian, albeit with a nonzero mean. The use of simple mean and rms statistics to characterize wind speed errors is thus warranted if the assumptions of Rayleigh distributed true wind speeds and the component noise error model (7) are valid.

4. Conditional means: Bias as a function of true wind speed

A major objective of validation analyses is to identify calibration and algorithm deficiencies that result in systematic errors in the derived geophysical data. Such errors are often manifested as biases that vary systematically with s. Unfortunately, it was shown in the previous section that random component errors can also yield overall biases, which may not be easily distinguishable from some forms of systematic calibration errors. It is thus useful to investigate conditional mean differences $\langle\Delta \mid s\rangle$ as functions of both s and component noise magnitude δ, to determine the extent to which random component noise might be incorrectly interpreted as systematic errors.

As in section 3, numerical simulations were used to investigate conditional mean differences. True wind speeds in realistic comprehensive validation datasets will be approximately Rayleigh distributed, and sample conditional means will thus have variable statistics as a function of s, owing to the relatively few observations corresponding to low or high true wind speeds. In the present analysis, $\langle\Delta \mid s\rangle$ was characterized separately for fixed values of s by generating realizations of true component speeds using (4) and adding Gaussian noise to the component speeds as in (6). Each simulation consisted of 1×10^5 noisy wind speed realizations corresponding to a single true wind speed s and component noise standard deviation δ. The full suite of simulations covered the parameter space $s = 0.1, 0.2, \ldots, 30$ m s^{-1} and $\delta = 0.5, 0.6, \ldots, 4.0$ m s^{-1}.

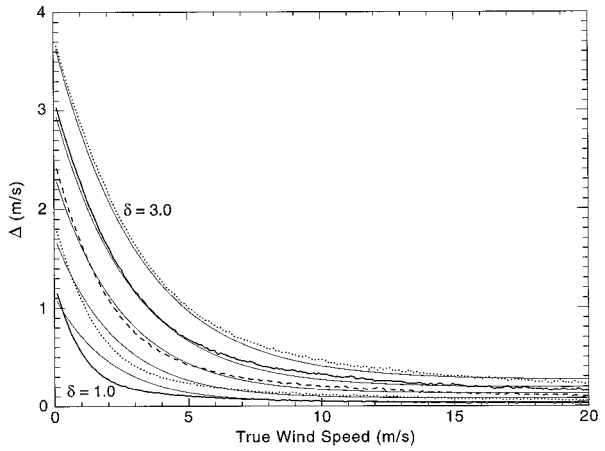

FIG. 3. Conditional mean differences ($\langle\Delta \mid s\rangle$) vs s derived from numerical simulations of the random-noise-only case for (bottom to top) $\delta = 1$, 1.5, 2, 2.5, and 3 m s^{-1} (heavy lines). Light solid lines are corresponding approximations from Eqs. (10a)–(10d).

Sample conditional mean differences are presented for selected values of δ in Fig. 3. Each of the parametric curves is nearly horizontal for large values of s, with $\langle\Delta \mid s\rangle$ increasing with increasing δ. More importantly, at low wind speeds the curves have increasingly (negative) slopes as s decreases or δ increases.

The nonlinear dependence of $\langle\Delta \mid s\rangle$ on s for $\delta \neq 0$ invalidates the use of simple straight-line fits for comparing collocated data, especially for low wind speeds. As with any analysis that fits a poor model to the data, the coefficients and other statistics resulting from the straight-line fit will be sensitive to the range of s used in the fit. While the curvature of $\langle\Delta \mid s\rangle$ in Fig. 3 decreases with increasing s and the slopes of straight-line fits of s_n to s approach the true value (unity) if the fits are restricted to large s, such restriction is generally ruled out in practice by the relative paucity of high wind speeds encountered in Rayleigh distributed validation datasets and by uncertainties in the accuracies of comparison measurements for extreme high wind conditions.

The simulation results suggest that the dependence of $\langle\Delta \mid s\rangle$ on s and δ for the random-noise-only case can be approximated by

$$\langle\Delta \mid s\rangle = A_1(\delta)e^{A_2(\delta)s} + A_3(\delta), \tag{10a}$$

where

$$A_1(\delta) = 1.04\delta + 0.038\delta^2 \tag{10b}$$

$$A_2(\delta) = -0.56 + 0.079\delta \tag{10c}$$

$$A_3(\delta) = 0.015\delta + 0.024\delta^2, \tag{10d}$$

and the coefficients were determined by nonlinear regression of (10a) on the numerical simulation results. As shown in Fig. 3, (10) is reasonably accurate at all wind speeds for $\delta > 1.5$ m s^{-1} and for $s > 4$ m s^{-1} for small δ. Thus, if it is known that $g(s) = s$, conditional mean difference data acquired over a range of s can in principle be regressed against (10) to estimate the variance of component random errors.

5. Linear systematic errors and random noise

The analyses presented in the previous section are valid only when it is known that the satellite wind speed measurements are contaminated solely by random noise (i.e., there are no systematic deterministic errors). Validation analyses more typically attempt to fit straight lines through raw or binned scatterplots, thereby implicitly assuming both systematic and random errors as in

$$s_n = \alpha_0 + \alpha_1 s + \epsilon \tag{11}$$

[i.e., $g(s) = \alpha_0 + \alpha_1 s$ in (4)]. It is necessary that $\alpha_n \geq 0$ in the noise-free case ($\delta^2 = 0$) to assure that s_n remains nonnegative for all $s \geq 0$. In practice, neither the scatterometer measurements nor the in situ comparison data are expected to be accurate at very low true wind speeds, and comparisons are often confined to cases in which s exceeds some threshold s_0. A low speed cutoff of $s_0 = 2$ m s^{-1} was used in the present study, leading to the restriction $\alpha_0 \geq -2\alpha_1$ to ensure $s_n \geq 0$, $s \geq 2$ m s^{-1}.

As in the random-noise-only case described in the previous section, numerical simulations were used to investigate conditional means and differences over the range $2 \leq s \leq 30$ m s^{-1}, $-2 \leq \alpha_0 \leq 2.3$ m s^{-1}, $0.7 \leq \alpha_1 \leq 1.3$, and $0 \leq \delta \leq 4$ m s^{-1}. Realizations of s_n were generated from true speeds by

$$s_{ni} = \{[(\alpha_0 + \alpha_1 s_i)\cos\theta_i + \delta_{1i}]^2 + [(\alpha_0 + \alpha_1 s_i)\sin\theta_i + \delta_{2i}]^2\}^{1/2}, \tag{12}$$

where α_0, α_1, δ, and s were constant for each simulation (1×10^5 realizations were generated per simulation), θ is a (uniformly distributed) random direction, and δ_1, δ_2 are independent $N(0, \delta^2)$ random component errors. The simulated conditional means for the scaled cases (α_0, $\alpha_1 \neq 0$) were qualitatively similar to those obtained for the random-noise-only case, although quantitative differences were found. The full set of simulations yielded a multidimensional tabulation of $\langle\Delta(s; \alpha_0, \alpha_1, \delta) \mid s\rangle$, which can be used in actual validation analyses as described in the following section.

6. Seasat and *ERS-1* scatterometer examples

In this section, the statistical validation analysis approach developed above is applied to collocated buoy-scatterometer datasets from both the Seasat and *ERS-1* missions.

The Seasat scatterometer (SASS) was a Ku-band (14.6 GHz) dual-swath scatterometer that flew on board the short Seasat mission in 1978. The SASS instrument and aspects of data processing are described in Bracalante et al. (1980), Woiceshyn et al. (1986), Chelton et

TABLE 1. Least squares parameters for the SASS and *ERS-1* buoy comparison datasets discussed in section 5. Here α_0, α_1 are deterministic offset and linear gain coefficients, respectively, and δ is the standard deviation of component errors from Eq. (12).

Dataset	Low wind speed cutoff (m s^{-1})	Nonlinear regression, Eq. (12)			Linear fit to sample means		Linear fit to unaveraged data	
		α_0 (m s^{-1})	α_1	δ (m s^{-1})	α_0 (m s^{-1})	α_1	α_0 (m s^{-1})	α_1
SASS	2	−1.3	1.03	1.8	−0.3	0.95	−0.3	0.94
	3	−0.9	1.00	1.3	−0.6	0.98	−0.5	0.96
	4	−0.8	1.00	0.5	−0.8	0.99	−0.6	0.97
ERS-1	2	−2.1	1.05	2.5	−0.1	0.91	0.1	0.87
	3	−2.0	1.04	2.5	−0.4	0.93	−0.1	0.88
	4	−2.0	1.04	2.5	−0.7	0.96	−0.4	0.92

al. (1990), and Naderi et al. (1991). Following the demise of Seasat in October 1978, several different vector wind datasets were produced using different model functions, wind retrieval algorithms, and spatial resolutions (see Chelton et al. 1990 for a brief review). Examples of historical wind speed validation analyses using collocated buoy and SASS data can be found in Woiceshyn et al. (1986), Freilich (1986), and references therein.

The present analysis examines SASS wind speed measurements and collocated neutral stability 19.5-m wind data derived from open-ocean operational meteorological buoys (cf. Freilich 1986). The SASS vector winds were calculated from vertically polarized backscatter measurements grouped into 100 km × 100 km regions, using the SASS-II model function (Wentz et al. 1984) and the maximum-likelihood wind retrieval estimator (Chi and Li 1988; Naderi et al. 1991). Each wind retrieval yields up to four vector solutions (''ambiguities'') having similar speeds but varying directions. The scatterometer wind speed was taken to be that of the ambiguity closest in direction to the collocated buoy wind vector.

Measurements from 28 buoys were used to calculate 19.5-m wind velocities for comparison with the SASS data. Whereas many previous validation investigations have simply compared SASS estimates with raw buoy anemometer data, the scatterometer measurements are thought to correspond to the equivalent neutral stability wind. Buoy measurements of wind speed at anemometer height (5 or 10 m for the buoys used here) as well as air and sea surface temperatures, surface pressure, and relative humidity data acquired by the buoys were used to calculate drag coefficents and 19.5-m neutral stability wind speeds based on the boundary layer model of Liu and Blanc (1984). The measured and 19.5-m neutral stability wind directions were assumed equivalent for the purpose of choosing the SASS ambiguity closest to the buoy direction.

The *ERS-1* Active Microwave Instrument (Attema et al. 1991) has been acquiring wind measurements since soon after its launch in July 1991. In scatterometer mode, it makes vertically polarized backscatter measurements at 5.3 GHz over a single, 500-km-wide swath using three fan-beam antennas oriented at 45°, 90°, and 135° with respect to the satellite ground track. As with the SASS instrument, several different model functions and processing algorithms have been used by different investigators to produce vector wind datasets (Freilich and Dunbar 1993; Offiler 1994). The validation technique is applied here only to the ''fast delivery'' dataset produced by ESA using the operational CMOD-4 model function (cf. Offiler 1994 and references therein).

The *ERS-1* scatterometer winds correspond to 10-m neutral stability winds (recall that SASS winds were 19.5-m altitude neutral stability winds). Comparison measurements were provided by a subset of 31 Northern Hemisphere extratropical operational meteorological buoys from the collocated *ERS-1*–buoy dataset assembled by Graber et al. (1996). Neutral stability winds at constant (10 m) altitude were calculated from the raw buoy data as described in Graber et al. (1996).

For both the SASS and *ERS-1* datasets, scatterometer and buoy measurements were collocated within a spatial window of 100 km and a temporal window of 30 min. Buoy measurements corresponding to wind speeds below 2 m s^{-1} or above 30 m s^{-1} were discarded, as were a small number of *ERS-1* scatterometer speed measurements less than 0.5 m s^{-1} or greater than 40 m s^{-1}. This editing yielded totals of 1024 and 3867 collocated wind speed pairs in the SASS and *ERS-1* datasets, respectively. Denoting the scatterometer wind speeds to be validated as s_n and the neutral stability wind speeds calculated from buoy measurements as s, sample conditional means $\langle s_n \mid s \rangle$ were calculated by binning all scatterometer measurements falling within 0.5 m s^{-1} ranges of s. (Note that $\langle \Delta \mid s \rangle = \langle s_n \mid s \rangle - s$.) To ensure stable and accurate sample statistics, sample conditional means used in the following analyses were calculated only for s bins containing 10 or more collocated pairs.

Three separate regression analyses were performed on each of the collocated datasets to estimate the deterministic coefficients α_i, with results presented in Table 1. A nonlinear least squares analysis regressed the sample conditional mean scatterometer speeds against the mean buoy speeds using the error model (12). For each set of parameters, the numerically generated sample conditional means calculated originally for equally

spaced values of s were interpolated to the sample mean buoy speeds. A comprehensive search of parameter space was then used to determine the values of α_0 (deterministic offset), α_1 (deterministic gain), and δ (component error standard deviation) yielding the minimum summed square deviation between the scatterometer sample conditional means and the numerically generated, interpolated conditional means.

Two ordinary least squares regression analyses were also performed for each of the datasets. In the first, the deterministic offset and gain were calculated by regressing the sample mean scatterometer speeds against the buoy mean speeds using a simple linear model. The second ordinary least squares analysis determined the α_i by regressing the raw (unaveraged) scatterometer measurements against collocated unaveraged 19.5-m (SASS) or 10-m (*ERS-1*) buoy speeds.

A common feature of both collocated datasets in Figs. 4a,b is the apparent relative insensitivity of the scatterometer measurements to buoy wind speed for mean buoy speeds less than about 5 m s^{-1}. This feature is found often in previously published comparisons and was attributed to fundamental model function errors by Woiceshyn et al. (1986) and Freilich (1986). Although the relationship between $\langle s_n \mid s \rangle$ and $\langle s \rangle$ is nearly linear for $s \geq 7$ m s^{-1}, the flattening of the relationship for small $\langle s \rangle$ will result in sensitivity of the coefficients calculated from strictly linear fits to the upper and lower buoy wind speeds used in the regressions. If the proposed noise model is correct, however, the best-fit coefficients from the nonlinear regression of sample means on simulated values from (12) should not be sensitive to the specific choice of the low wind speed cutoff. All three regression methods were therefore used to calculate coefficients for low wind speed cutoffs ranging from 2 to 4 m s^{-1} (Table 1). As expected, in both the SASS and *ERS-1* analyses the best-fit line coefficients (from ordinary linear least squares regressions) varied significantly as a function of low wind cutoff, with α_0 becoming more negative and α_1 approaching unity as the cutoff speed was increased. As shown by the heavy solid lines in Figs. 4a,b, best-fit coefficients from the nonlinear noise model (12) resulted in low wind flattening qualitatively similar to that observed in the data. The nonlinear best-fit coefficients were virtually insensitive to the choice of low-wind cutoff for the *ERS-1* dataset. In the nonlinear SASS analysis, the coefficients depended on the low-wind cutoff used in their calculation, suggesting either that the SASS measurements at low wind speeds are corrupted by other errors in addition to the noise modeled in this study or that the development and tuning of the SASS-II v-pol model function resulted in (mildly) corrupted estimates at both low- and midrange wind speeds.

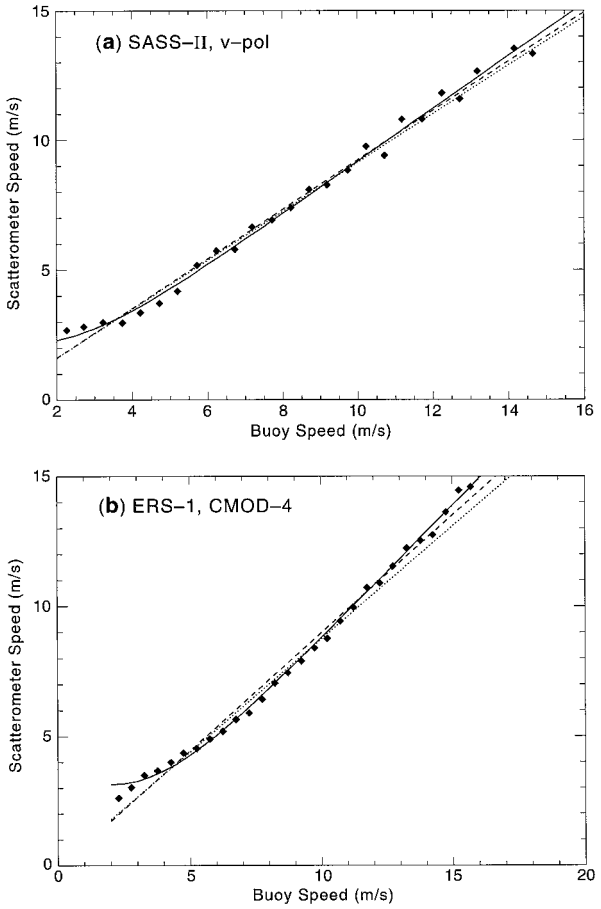

FIG. 4. Sample scatterometer conditional mean speeds (diamonds), least squares result from the nonlinear analysis of section 5 (heavy solid line), ordinary least squares line fit to the sample means (dashed line), and ordinary least squares line fit to the raw (unaveraged) scatterometer–buoy scatterplot (dotted line). Sample conditional means were calculated only for 0.5 m s^{-1} bins containing at least 10 collocated pairs and for mean buoy speeds exceeding 2 m s^{-1}. (a) Seasat scatterometer measurements (SASS-II model function, vertical polarization). (b) *ERS-1* scatterometer measurements (CMOD-4 model function, vertical polarization).

7. Discussion and conclusions

A consistent analysis approach has been developed for validating satellite wind speed measurements using collocated in situ or previously calibrated comparison data. It has been assumed throughout that the comparison data are error free. The new validation approach differs from most previous analyses in its explicit recognition that all physically realistic wind speeds (both true and noisy) must be nonnegative.

A noise model (12) was developed for the case where the satellite measurements were contaminated by both linear deterministic calibration errors and additive, normally distributed random errors on each component. It was shown analytically that this noise model results in Rayleigh distributed noisy wind speeds in the random-noise-only case (7) if the true winds are themselves Rayleigh distributed. However, the overall mean wind speed for the noisy dataset is different from the corresponding mean true wind speed, owing to the additional component variability resulting from the noise. The

presence of random errors thus leads to overall wind speed biases.

Numerical simulations were used to investigate second-order statistics of the differences between noisy and true wind speeds. For the globally realistic case of Rayleigh distributed true wind speeds with $\bar{s} = 7.4$ m s^{-1}, overall rms differences were found to be accurately approximated by the standard deviation of the component noise, and the population distribution of noisy minus true speed differences was nearly Gaussian.

The effects of the nonnegative constraint on noisy wind speeds were most apparent in the investigation of conditional mean speed differences. Numerical simulations demonstrated clearly that conditional mean differences are nonlinear functions of true speed, and thus simple straight-line fits between conditional mean satellite-measured speeds and true speed will not yield useful information and can lead to erroneous interpretations. The numerical simulations were used to quantify conditional mean differences as functions of true wind speed, random noise magnitude (standard deviation of the normally distributed additive component noise), and deterministic gain and offset [cf. (10) and section 5] for a wide range of realistic parameter values.

The numerical results were then applied to actual validations involving collocations of Seasat and *ERS-1* scatterometer data with extensive sets of operational meteorological buoys. Buoy measurements were transformed to 19.5-m (Seasat) and 10-m (*ERS-1*) neutral stability wind speeds, and sample mean satellite wind speeds were calculated for 0.5 m s^{-1} bins defined by the buoy measurements. A straightforward nonlinear least squares approach was used to determine the offset, gain, and noise magnitude values for each dataset by regression of the measured values against the previously calculated conditional means from numerical simulations.

Simple straight-line fits typical of previous (incorrect) validation analyses yielded best-fit gains less than unity and small offsets for both the Seasat and *ERS-1* datasets, although detailed coefficient values were sensitive to the precise low wind speed cutoffs used in the analysis. The more correct validation approach developed in this study resulted in best-fit gains very near unity, negative deterministic offsets, and realistic noise magnitudes for each dataset. The coefficient estimates from the new validation approach were nearly insensitive to changes in the low wind speed cutoffs.

An apparent low wind speed insensitivity of scatterometers has been observed in many validation studies (Woiceshyn et al. 1986; Freilich 1986), and it is present in both the SASS and *ERS-1* comparison datasets analyzed here. On dynamical grounds, Donelan and Pierson (1987) postulated the existence of a low true wind speed cutoff, below which scatterometer backscatter measurements would drop rapidly to zero. However, such a cutoff has never been observed in spaceborne data, and the feature in Figs. 4a,b has the opposite sense to that suggested by Donelan and Pierson. Wentz and coworkers (Wentz et al., 1984; Chelton and Wentz 1986) suggested that the observed feature might result from errors in the comparison (buoy) measurements. Such an explanation cannot be ruled out by the present analysis, since it has been assumed that the buoy measurements are perfect. However, the ability of the present analysis to model the observed results suggests that random component errors in the remotely sensed data play a far more significant role than was heretofore suspected.

The present analysis raises questions regarding proper instrument calibration and algorithm refinement when it is known that the vector magnitude data to be validated contain significant random errors. Random component errors introduce positive wind speed biases at all true wind speeds, although the effect is greatest at low true winds. Both the SASS and *ERS-1* wind speed regressions suggested a deterministic negative wind speed bias as well as significant random component errors. It is likely that the instrument calibrations and model functions originally used to process the data were unwittingly and incorrectly tuned by others to remove portions of the overall wind speed bias contributed by random component errors.

As noted in the introduction, certain random errors could be manifested as speed biases even for instruments that measure only wind speeds (or other vector magnitudes), as long as the processing algorithms are constrained to produce only physically realistic nonnegative speeds. While detailed analyses are beyond the scope of the present paper, Boutin and Etcheto (1996) recently reported that Geosat altimeter wind speeds are biased high relative to tropical buoy measurements for buoy-measured speeds lower than 4 m s^{-1}. Similar comparisons of remotely sensed wind speeds with ship measurements reported by Boutin and Etcheto (1996; their Fig. 1) suggest both an overprediction and a relative insensitivity of the remotely sensed wind speeds to the collocated ship-measured speeds at low wind speeds. However, care must be taken when analyzing these results, as it is known that errors in the ship wind speed measurements (neglected in the present analysis) can be substantial, unreported systematic gain and offset errors may be present in the remotely sensed measurements, and neither the altimeter nor the microwave radiometer wind speed algorithms preclude negative wind speeds as required by the present approach.

The magnitude and wind speed dependence of the wind speed bias is largest at low true wind speeds, and it is apparent that the incorrect standard validation and model function tuning techniques will be sensitive to both the relative proportion of low wind speeds in the comparison dataset and the magnitude of the noise. The extensive Tropical Atmosphere–Ocean (TAO) array of low-latitude buoys (Hayes et al. 1991) provides many opportunities for collocations between satellite and in situ wind measurements. These data are proving invaluable for detailed validation of present and future

satellite instruments. However, the mean tropical wind speed is significantly lower than the global mean, and collocations with TAO measurements include far more low winds than do collocations with midlatitude buoys. Errors introduced by overly simplistic validation analyses (such as ordinary least squares straight-line fits) will be more significant when satellite measurements are compared with TAO data than with midlatitude or global buoy datasets.

The nonlinear validation approach developed here accounts properly for the dependence of random component error bias on true wind speed and furthermore provides a direct estimate of component noise magnitude in addition to the more standard estimates of deterministic gain and offset.

Acknowledgments. Drs. Hans Graber and Naoto Ebuchi graciously supplied an advance copy of the collocated *ERS-1*–buoy dataset. The *ERS-1* scatterometer data were provided by the European Space Agency, and the Seasat SASS data were obtained from the Physical Oceanography DAAC at JPL. Dudley Chelton, David Long, and an anonymous reviewer contributed helpful comments. This work was supported in part by the NASA Physical Oceanography Program through Grants NAGW-3062 and NAGW-3615 to Oregon State University and by the JPL NSCAT Project through Contract 959351.

REFERENCES

Abramowitz, A., and I. A. Stegun, 1964: *Handbook of Mathematical Functions.* Dover, 1046 pp.

Attema, E. P. W., 1991: The active microwave instrument on board the ERS-1 satellite. *Proc. IEEE,* **79,** 791–799.

Boutin, J., and J. Etcheto, 1996: Consistency of Geosat, SSM/I, and *ERS-1* global surface wind speeds—Comparison with in situ data. *J. Atmos. Oceanic Technol.,* **13,** 183–197.

Bracalante, E. M., D. H. Boggs, W. L. Grantham, and J. L. Sweet, 1980: The SASS scattering coefficient algorithm. *J. Oceanic Eng.,* **OE-5** (2), 145–154.

Chelton, D. B., and F. J. Wentz, 1986: Further development of an improved altimeter wind speed algorithm. *J. Geophys. Res.,* **91,** 14 250–14 260.

——, A. M. Mestas-Nunez, and M. H. Freilich, 1990: Global wind stress and Sverdrup circulation from the Seasat scatterometer. *J. Phys. Oceanogr.,* **20,** 1175–1205.

Chi, C.-Y., and F. K. Li, 1988: A comparative study of several wind estimation algorithms for spaceborne scatterometers. *IEEE Trans. Geosci. Remote Sens.,* **GE-26,** 115–121.

Donelan, M. A., and W. J. Pierson, 1987: Radar scattering and equilibrium ranges in wind-generated waves with application to scatterometry. *J. Geophys. Res.,* **92,** 4971–5029.

Essenwanger, O., 1976: *Applied Statistics in Atmospheric Science. Developments in Atmospheric Science,* Vol. **4A**, Elsevier, 412 pp.

Freilich, M. H., 1986: Satellite scatterometer comparisons with surface measurements: Techniques and Seasat results. *Proc. Workshop on ERS-1 Wind and Wave Calibration,* Schliersee, Germany, ESA, ESA SP-262, 57–62.

——, and R. S. Dunbar, 1993: A preliminary C-band scatterometer model function for the ERS-1 AMI instrument. *Proc. First ERS-1 Symp.,* Cannes, France, ESA, ESA SP-359, 79–83.

——, and P. G. Challenor, 1994: A new approach for determining fully empirical altimeter wind speed model functions. *J. Geophys. Res.,* **99,** 25 051–25 062.

Graber, H. C., N. Ebuchi, and R. Vakkayil, 1996: Evaluation of ERS-1 scatterometer winds with wind and wave ocean buoy observations. University of Miami Tech. Rep. RSMAS 96-003, 78 pp. [Available from Prof. Hans Graber, RSMAS/AMP, 4600 Rickenbacker Causeway, Miami, FL 33149.]

Hayes, S. P., L. J. Magnum, J. Picaut, and K. Takeuchi, 1991: TOGA-TAO: A moored array for real-time measurements in the tropical Pacific Ocean. *Bull. Amer. Meteor. Soc.,* **72,** 339–347.

Justus, C. G., W. R. Hargraves, A. Mikhail, and D. Graber, 1978: Methods for estimating wind speed frequency distributions. *J. Appl. Meteor.,* **17,** 350–353.

Liu, W. T., and T. V. Blanc, 1984: The Liu, Katsaros, and Businger (1979) bulk atmospheric flux computational iteration program in FORTRAN and BASIC. NRL Memo. Rep. 5291, 16 pp. [Available from Naval Research Laboratory, Code 4110, Washington, DC 20375.]

Monaldo, F., 1988: Expected differences between buoy and radar altimeter estimates of wind speed and significant wave height and their implications on buoy-altimeter comparisons. *J. Geophys. Res.,* **93,** 2285–2302.

Naderi, F. M., M. H. Freilich, and D. G. Long, 1991: Spaceborne radar measurement of wind velocity over the ocean—An overview of the NSCAT scatterometer system. *Proc. IEEE,* **79,** 850–866.

Offiler, D., 1994: The calibration of *ERS-1* satellite scatterometer winds. *J. Atmos. Oceanic Technol.,* **11,** 1002–1017.

Parzen, E., 1960: *Modern Probability Theory and Its Applications.* John Wiley and Sons, 464 pp.

Pavia, E. G., and J. J. O'Brien, 1986: Weibull statistics of wind speed over the ocean. *J. Climate Appl. Meteor.,* **25,** 1324–1332.

Pierson, W. J., 1983: The measurement of the synoptic scale wind over the ocean. *J. Geophys. Res.,* **88,** 1683–1708.

Press, W. H., S. A. Teukolsky, W. T. Vettering, and B. P. Flannery, 1992: *Numerical Recipes in FORTRAN.* 2d. ed. Cambridge University Press, 963 pp.

Stewart, D. A., and O. M. Essenwanger, 1978: Frequency distribution of wind speed near the surface. *J. Appl. Meteor.,* **17,** 1633–1642.

Takle, E. S., and J. M. Brown, 1978: Note on the use of Weibull statistics to characterize wind-speed data. *J. Appl. Meteor.,* **17,** 556–559.

Wentz, F. J., S. Peteherych, and L. A. Thomas, 1984: A model function for ocean radar cross sections at 14.6 GHz. *J. Geophys. Res.,* **89,** 3689–3704.

Woiceshyn, P. M., M. G. Wurtele, D. H. Boggs, L. F. McGoldrick, and S. Peteherych, 1986: The necessity for a new parameterization of an empirical model for wind/ocean scatterometry. *J. Geophys. Res.,* **91,** 2273–2288.